La_2O_3 AS PRIMER FOR SUPPORTING $La_{0.9}Ce_{0.1}CoO_{3\pm\delta}$ ON CORDIERITIC HONEYCOMBS

L. Fabbrini, I. Rossetti, L. Forni*

Dipartimento di Chimica Fisica ed Elettrochimica, Università degli Studi di Milano

via C. Golgi, 19, I-20133 Milano, Italy

ABSTRACT

To better understand the effect of La_2O_3 as primer for the preparation of honeycomb supported $La_{0.9}Ce_{0.1}CoO_{3\pm\delta}$ catalyst, some sample were prepared starting from different La-precursors. Physical and morphological properties of both the primer-coated honeycomb and its precursors (as prepared and after thermal treatment at different temperature) have been investigated by TGA, TPD-MS, XRD and SEM. Calcination at high temperature brought about a rearrangement of both primer and active phase morphology. When La acetate was used as precursor, such a transformation seemed not to alter substantially the morphology of the primer layer, leading to a poorer anchoring to the support, with deep cracking and exfoliation of the La oxide platelets so formed. By contrast, when the primer precursor was La nitrate, the higher reactivity of the hydroxynitrates, forming during calcination, with respect to both the active phase and the honeycomb, led to a more uniform and compact La_2O_3 layer, anchoring much better the perovskite to the monolith support.

Keywords: methane, catalytic combustion; lanthanum oxide; perovskite supporting on honeycomb monoliths

**Corresponding Author: fax: +39-0250314300; e-mail: lucio.forni@unimi.it*

1. INTRODUCTION

The abatement of gaseous pollutants such as NOx, CO and un-burned hydrocarbons is of ever-growing concern for environment protection. Perovskitic mixed oxides proved since long time to be a valuable alternative to the traditional noble metal based catalysts for many of these reactions, being cheaper, comparatively active and thermally stable, if properly prepared [1,2]. In particular, $La_{0.9}Ce_{0.1}CoO_{3\pm\delta}$ showed very active for the complete flameless combustion of hydrocarbons [3-5].

For practical application, structured catalysts are the most used, in order to reduce substantially the pressure drop across the catalyst bed. Usually structured catalysts are prepared by deposition of the active phase on cordieritic honeycomb monoliths. To favour the adhesion of the active phase to the support, the latter is usually pre-coated with a primer, whose function is also to increase the surface area and to improve catalyst stability [6]. One of the most commonly used primer materials is γ-Al_2O_3, which however in some cases does not ensure a sufficient stability. The latter can be improved either by doping the alumina or by using different mixed oxides, such as Zr-Ce-Ti-Mg-O [7,8].

In a previous work [5] it was shown that $La_{0.9}Ce_{0.1}CoO_{3\pm\delta}$ cannot be firmly anchored onto a honeycomb monolith in the absence of a primer. Furthermore, alumina did not ensure a good thermal resistance to supported lanthanum cobaltites, due to the formation of $LaAlO_3$ or $CoAl_2O_4$, progressively leading to the destruction of the active phase during high temperature use of the catalyst. Moreover, alumina itself easily sinters, so reducing catalyst surface area. Finally, its different thermal dilatation coefficient with respect to the cordieritic support can be very likely the main cause of the formation of deep cracks in the coating [5].

A valid alternative primer for the present application showed La_2O_3, which can be deposited from different precursors. A slightly higher activity was obtained with lanthanum

oxide prepared from lanthanum acetate, but a much higher thermal resistance was observed using lanthanum nitrate as precursor [5].

The aim of the present work was to investigate the reason of the different behaviour of these primer precursors. For this purpose, four honeycomb supported $La_{0.9}Ce_{0.1}CoO_{3\pm\delta}$ samples were prepared, in which the La_2O_3 primer was prepared from either acetate or nitrate. Physical and morphological properties of primer, precursor and finished catalyst have been analysed by TGA, TPR-TPD-MS, XRD and SEM, before and after thermal treatment at different temperatures. At last the catalysts have been compared under identical reaction conditions for the catalytic flameless combustion (CFC) of methane, before and after several cycles of reaction/accelerated deactivation.

2. EXPERIMENTAL

2.1. Active phase preparation

$La_{0.9}Ce_{0.1}CoO_{3+\delta}$ was prepared by the flame hydrolysis (FH) technique. A detailed description of the apparatus can be found elsewhere [3]. Briefly, the preparation started from a 3% aqueous solution of precursors ($La(NO_3)_3{\bullet}6H_2O$, Aldrich, purity ≥99.99%; $Ce(NO_3)_3{\bullet}6H_2O$, ACROS, purity ≥ 99.50%; $Co(NO_3)_2$, Merck, purity ≥ 99.99%). Citric acid (Aldrich, purity ≥99.0%) was added both as complexing agent and as additional fuel to increase the flame temperature. The solution was nebulised into a H_2+O_2 flame and the perovskite powder was collected by means of an electrostatic precipitator.

The high temperature (*ca*. 1600°C) attained in the flame allowed to obtain a very high phase purity and satisfactory thermal resistance of both the powder and the supported catalyst. Moreover, the very short residence time within the flame [3,5] limited any extended sintering of the powder, leading to relatively high BET surface area (*ca*. 20

m^2/g). SEM analysis showed clusters, 200-500 nm in size, made of highly uniform, nearly spherical particles, 20-80 nm in size.

2.2. Primer precursors treatment

Samples of La oxide from La nitrate and La acetate in powder form (La-N-500, La-N-700, La-Ac-500, La-Ac-700, Table 1) were obtained by calcination at either 500°C or 700°C for 1 h.

2.3. Primer and active phase deposition on honeycomb monoliths

For the wash-coat deposition of the primer from $La(CH_3COO)_3 \bullet H_2O$, which is scarcely soluble in water (0.17 g/l at 25°C [9]), a stable suspension of 1.5 g of salt in 22.5 cm^3 of distilled water was obtained by ball-milling for 2 h in a tumbling 50 cm^3 cylindrical polypropylene jar with five zirconia balls (D=10 mm).

The high solubility of $La(NO_3)_3 \bullet 6H_2O$ allowed to prepare a clear and stable solution, by dissolving 3 g of salt in 22.5 ml of distilled water. The molar concentration of lanthanum (*ca*. 10^{-4} M) in the starting solution/suspension, allowed to obtain the deposition of up to 2 wt % of La_2O_3 from acetate and 4 wt % from nitrate, during each dip-coating step.

A detailed description of the apparatus and the conditions adopted for the dip-coating can be found elsewhere [5]. Briefly, a cylindrical monolith, 1 cm diameter x 5 cm length, obtained from a commercial cordieritic honeycomb ($Mg_2Al_3(AlSi_5O_{18})$, 400 cpi = 62 cells/cm^2, wall thickness = 0.15 mm) was calcined at 500°C for 1 hour and weighed. The dip-coating was accomplished by means of a home made apparatus, so to dip and withdraw, at the desired constant speed, the honeycomb from the solution/suspension. Every dipping was followed by drying at room temperature for 10 min. After deposition of the primer precursors the samples were calcined at 500 or 700°C in air for 1 h. The deposition of the active phase was carried out by dip-coating the primer-coated monolith

with a suspension of the perovskite powder. The latter was obtained by ball-milling 0.8 g of the FH prepared $La_{0.9}Ce_{0.1}CoO_{3+\delta}$ powder in 20 cm^3 of distilled water for 4h. Finally, the samples were calcined at 500°C for 1 h.

Primer and active phase loading was expressed as weight percent referred to the final catalyst weight. The composition of the prepared catalysts is given in Table 1 (sample H-N-500, H-N-700, H-Ac-500 and H-Ac-700).

2.4. Sample characterisation

Thermogravimetric analysis of the primer precursors powder was carried out in flowing air or N_2 by means of a Perkin Elmer TGA7 apparatus. Temperature ramp was 2°C/min from 50 up to 900°C. TPD-TPR/MS analysis was performed in flowing helium, while increasing temperature by 10°C/min from 50 up to 800°C. A detailed description of the apparatus was given elsewhere [10]. XRD analysis was carried out on a Philips PW 1820 diffractometer, using the Ni-filtered Cu Kα radiation (λ = 0.15418 nm). Phase recognition was done by comparison with literature data [11]. A Cambridge Stereoscan 150 scanning electron microscope (SEM) was employed for morphological analysis of the calcined precursor salts of the deposed primer layer and of the final catalyst.

2.5. *Catalytic activity*

The catalytic activity tests for the CFC of methane were carried out by means of a bench-scale continuous reactor. An Incoloy 800 tubular reactor, 400 mm in length and i.d. = 10.5 mm, was put within two heavy metal blocks into a tubular furnace. The honeycomb was placed in the isothermal middle part of the reactor, between two flocks of quartz wool. The void part of the reactor tube, above and below the catalyst bed, was filled with quartz beads (10-20 mesh). Prior to each run, the catalyst was activated in flowing air (20 cm^3/min), while increasing temperature by 10°C/min up to 600°C, then kept for 1 h. The

activity tests were carried out by feeding a mixture composed of 0.5 vol% CH_4, 49.5 vol% He and 50 vol% air, while increasing temperature by 2°C/min from 250 up to 600°C. The outlet gas was analysed in line by means of an HP 5890 gas chromatograph. The total flow rate of the mixture was calculated by referring to the mass of active phase, so to have for every test an identical value of the time factor τ = W/F=2.5 mg of perovskite min/cm^3 of overall gas flow rate.

2.6. Accelerated thermal deactivation tests

Accelerated thermal deactivation tests were carried out after keeping the sample at the temperature (T_f) of maximum conversion, for 24 h. Then cycles of reaction/deactivation were accomplished by increasing temperature (10°C/min) up to 800°C, kept for 1 h. The temperature was then brought back to T_f, kept for 3 h, during which the catalytic activity was measured. The cycles were repeated, till a decrease in conversion at T_f was noticed.

3. RESULTS AND DISCUSSION

In our previous investigation we concluded that La-oxide can be a valuable alternative to alumina from both the points of view of catalytic activity and thermal stability. However, we noticed a different grafting ability when the La-oxide layer was prepared from acetate or nitrate as precursor. In particular, during our accelerated deactivation tests, the best thermal resistance was obtained by using the nitrate, calcined at 500°C, as primer precursor.

3.1. *Characterisation of La-acetate and La-nitrate powders*

Thermogravimetric analysis showed that lanthanum acetate looses weight during three different steps (Fig.1a). The most evident step took place between 300 and 400°C,

with *ca*. 45% weight loss. TPD-MS analysis, carried out in inert atmosphere under the same conditions of the TGA experiments, showed that the first step (at *ca.*150°C) was due to loosing of crystallisation water. The second step (between 300 and 400°C) corresponded to the release of acetone ("A" in the Figure) and CO_2. The third step, between 600° and 700°C, was ascribable to the release of CO_2. The loss of acetone could take place through the following possible reaction path, involving the intermediate formation of lanthanum oxide-carbonate La_2CO_5 [11,12]:

$$2La(CH_3COO)_3 \rightarrow La_2(CO_3)_3 + 3CH_3COCH_3$$

$$La_2(CO_3)_3 \rightarrow La_2CO_5 + 2CO_2$$

Finally, by further heating at 650°C, lanthanum oxide-carbonate decomposes into La_2O_3, with emission of CO_2.

Lanthanum nitrate is a very hygroscopic salt, containing six molecules of crystallisation water. During heating the salt releases first part of the water at low temperature (50-100°C). Above 50°C the salt melts and recombines in the remaining water [12]. The product so formed undergoes a complex series of decomposition steps, leading to the completely water free La_2O_3 at T>650°C only (Fig.1b). The TPD-MS analysis of lanthanum nitrate evidenced that the salt releases gradually the crystallisation water during the whole temperature ramp. The greatest peak, between 300 and 400°C, corresponds to the release of NO, N_2O and NO_2. At higher temperature (>600°C) the sample releases the residual water only, until the formation of the anhydrous lanthanum oxide.

XRD analysis (Fig.2a and 2b) confirmed the previously suggested decomposition mechanisms. Indeed, after calcination at 500°C the acetate formed the La-oxide-carbonate (La_2CO_5) [11], while lanthanum nitrate formed a mixture of basic hydroxynitrates [12], such as $La(OH)_2(NO_3)$, $La_2(OH)_{5.1}(NO_3)_{0.9}$ [11]. All the intermediates forming from any of the

precursors transform into La_2O_3 [11] when treated at 700°C (upper temperature pattern of both Fig.2a and 2b).

A further interesting information derived from SEM analysis. Micrographs of the calcined powdered precursors (Fig. 3) showed that acetate doesn't change appreciably its morphology when calcined at either 500 or 700°C, in spite of the evident change of crystalline structure (Fig.2). In both samples it appeared in the form of micro-particles with irregular shape. The main difference between samples La-Ac-500 (Fig.3a) and La-Ac-700 (Fig.3b) was the more compact structure of the former, with some cracks on the particle surface, while La-Ac-700 showed deeper and larger cracks. Moreover, Fig.3c and 3d showed that the hydroxynitrates, forming during the decomposition of the nitrate at 500°C, possess a markedly different morphology whit respect to the La_2O_3 obtained at 700°C. Indeed, La-N-500 (Fig.3c) showed needle-shaped particles agglomerates, while La-N-700 showed laminar multilayers (Fig.3d). Finally, it is also important to notice the deeply different morphology of the La_2O_3 obtained from the two precursors (Fig.3b and 3d). It is reasonable to suppose that the decomposition of the acetate, taking place with evolution of gaseous CO_2 and acetone, favours the sample sintering and cracking. By contrast, the peculiar decomposition mechanism of the nitrate, involving both melting and recombination steps, leads to a more uniform and compact structure.

3.3. Primer-coated monoliths

As for the phase composition of the supported samples, unfortunately, due to coating thickness and amount with respect to the support it was impossible to analyse it directly through XRD. However, a sort of simulation was carried out by finely mixing powders of the primer precursor and of the active phase in proper amounts. The mixture was then calcined at 600 and 800°C in order to simulate thermal treatments of the catalyst during activity and deactivation tests. XRD analysis confirmed that upon treatment at

600°C the perovskitic phase coexists with a mixture of La_2O_3 and lanthanum hydroxynitrates. When heated at 800°C it was observed a complete decomposition of the hydroxynitrates to lanthanum oxide.

SEM micrographs (before the deposition of the active phase) of sample H-Ac-500 (Table 1) showed small platelets, uniformly distributed on the support (Fig. 4a). Further calcination at 700°C led to platelets agglomeration into larger plates, easily detachable from the support (sample H-Ac-700, Fig.4b). The morphology of sample H-N-500 was completely different, resembling a sort of needle carpet (Fig.4c). After calcination at 700°C the latter transformed into nearly spherical particles, partly agglomerated into larger clusters, more or less uniformly distributed over the honeycomb surface (sample H-N-700, Fig.4d).

The present data support the findings of our previous paper [5], about the better priming action of the La-nitrate-derived La-oxide primer and help in throwing light on such a different behavior. Indeed, when lanthanum acetate progressively transforms into the oxide, the morphology of the latter prevents a perfect grafting onto the monolith surface. Furthermore, high temperature calcination not only does not modify appreciably the morphology of the primer layer, but also favors the cracking and exfoliation of the La_2O_3 platelets. By contrast, the intermediate material, forming from the nitrate precursor calcined at 500°C, anchors much better to the monolith surface. After calcination at 700°C this intermediate leads to La_2O_3 possessing a morphology much more favorable for grafting, consisting in microspheres firmly anchored to the support.

The subsequent deposition of the perovskite on the primer prepared from acetate and calcined at 500°C leads to two overlapping distinct layers, the lower one made of La_2CO_5 and the upper one of perovskite. Calcination at 700°C causes the further transformation of the oxide-carbonate into La_2O_3, with partial sintering into larger platelets and more severe cracking, but without any substantial change in the grafting ability of the

primer. This reflects on catalytic activity (samples H-Ac-500 and H-Ac-700, Fig.5), which slightly decreased after primer sintering. However, the main consequence can be observed on thermal resistance, which strongly decreased on heating (Fig.6).

By contrast, when the active phase is deposed on the support coated with the nitrate precursor calcined at 500°C (sample H-N-500), a stronger grafting action takes place. Indeed, during reaction and especially during the high temperature accelerated deactivation cycles, the complete transformation of the primer precursor into La_2O_3 leads to the formation of a much more compact primer layer, grafting both the cordierite and the active phase and leading to excellent thermal stability. However, when the active phase is deposed on the primer-coated monolith calcined at 700°C (H-N-700), the more sintered primer particles do not ensure the same good grafting action as for sample H-N-500. As a consequence, thermal resistance remains slightly lower, as evidenced by the stability test (Fig.6).

At last, the set of SEM micrographs (Fig.7), collected at the end of the accelerated catalyst deactivation tests (Fig.6), further supported our interpretation. Indeed, La oxide primer from acetate confirmed to possess the worst grafting ability at both calcination temperatures, leading to the formation of much deep cracks and to exfoliation of the deposed perovskite layer (Fig.7a,b). The only sample maintaining a compact active phase layer, firmly anchored to the support, was H-N-500, with primer from La nitrate calcined at 500°C (Fig.7c). Calcination of the same primer precursor at 700°C (Fig.7d) brought about the formation of a less compact layer, characterised by larger holes and leading to a worse distribution of the active phase, in spite a good grafting to the support.

Of course, activity decrease after thermal deactivation can also be ascribed to a more or less evident loss of active phase. Unfortunately, the weight loss during prolonged activity testing is hardly detectable due to different reasons. First of all, further primer decomposition upon heating causes weight loss ascribable to elimination of CO_2, H_2O or

NOx, depending on the primer precursor, as clearly evidenced by our TGA experiment (*vide supra*). This phenomenon has to be added to a possible weight loss due to catalyst powder detachment. Since the amount of active phase loaded onto the monolith is ca. 50-60 mg for each sample, the loss of catalyst powder can be hardly distinguishable. Moreover, coating detachment involves both the primer and the active phase, further complicating the quantification of catalyst loss and hence any correlation with activity decrease. In spite of these difficulties we tried to quantificate catalyst detachment by loading 2 wt% of $La_{0.9}Ce_{0.1}CoO_3$ on the monolith surface without any primer. In this way we would obtain less adhesion of the catalyst on the support and hence observe, after the thermal deactivation cycles, an amount of powder detached which will be an upper limit for the primer coated sample. This test indicated an active phase loss lower than 5 wt%.

4. CONCLUSIONS

Heating up to high temperature brings about a rearrangement of the as-deposed primer layer structure, involving also the overlying active phase layer. La oxide platelets from acetate, being much less reactive with the honeycomb surface, coalesce, crack and exfoliate since the calcination preceding the deposition of the perovskite. By contrast, the higher reactivity, towards both the active phase and the honeycomb, of the hydroxy-nitrates needles, forming at 500°C, seems the major parameter to be governed for obtaining a more uniform and compact La oxide layer, anchoring much better the perovskite to the support.

REFERENCES

1. Y. Teraoka, H. Fukuda, S. Kagawa, Chem. Lett., 1 (1990) 1.
2. M.A. Peña, J.L.G. Fierro, Chem. Rev., 101 (2001) 1981.
3. R. A. M. Giacomuzzi, M. Portinari, I. Rossetti, L. Forni, *Stud. Surf. Sci. And Catal*., A. Corma, F.V. Melo, S. Mendioroz, J.L.G. Fierro, Eds., Vol. 130, Elsevier, Amsterdam, 2000, p.197.
4. L. Forni, I. Rossetti, Appl. Catal. B: Environ. 38 (2002) 29.
5. L. Fabbrini, I. Rossetti, L. Forni, Appl. Catal. B: Environ. 44 (2003) 107.
6. E. Tronconi, Chim. Ind. (Milan), 81 (1999) 875.
7. M.F.M. Zwinkels, O. Haussner, P. Govind Menon, S.G. Jaras, Catal. Today, 47 (1999) 73.
8. M.J. Andrews, M.K. Ferber, E. Lara-Curzio, J. Eur. Ceram. Soc., 22 (2002) 2633.
9. P. Pascal, Noveau Traité de Chimie Minérale, Ed. Masson et C^{ie}, Paris, 1959, Vol. VII, p. 1000.
10. L. Forni, M. Toscano, P. Pollesel, J. Catal., 130 (1991) 392.
11. Selected Powder Diffraction Data, J.C.P.D.S., Swarthmore, PA, Minerals, Files no. 23-0322 (La_2CO_5), 26-1146 ($La(OH)_2NO_3$), 26-1145 ($La_2(OH)_{5.1}NO_{0.9}$), 05-0602 (La_2O_3).
12. T. Moeller, V. D. Aftandilian, J. Am. Chem. Soc., 76 (1954) 5249.

Table 1: Catalyst composition

SAMPLE	PRIMER PRECURSOR	wt % of primer and of active phase	calcination T (°C) of primer
La-N-500	La-nitrate	/	500
La-N-700	La-nitrate	/	700
La-Ac-500	La-acetate	/	500
La-Ac-700	La-acetate	/	700
H-N-500	La-nitrate	4% and 2%	500
H-N-700	La-nitrate	4% and 2%	700
H-Ac-500	La-acetate	2% and 2%	500
H-Ac-700	La-acetate	2% and 2%	700

FIGURE CAPTIONS

Fig. 1: Thermogravimetric analysis of lanthanum acetate (a) and nitrate (b). A = acetone.

Fig. 2: XRD patterns of La-oxide intermediates obtained from (a) La acetate and (b) La nitrate, calcined at different temperatures. Upper pattern of both the Figures: La_2O_3 (JCPDS file 05-0602). Lower pattern of Fig.a: La_2CO_5 (JCPDS file 23-0322); lower pattern of Fig.b: mixture of $La(OH)_2NO_3$ (JCPDS file 26-1146) and $La_2(OH)_{5.1}(NO_3)_{0.9}$ (JCPDS file 26-1145).

Fig. 3: Typical SEM micrographs of primer precursors from La acetate powder calcined at 500°C (a) and 700°C (b) and from La nitrate powder calcined at 500°C (c) and 700°C (d)

Fig. 4: Typical SEM micrographs of primer-coated honeycomb monoliths walls. Sample H-Ac-500 (a), H-Ac-700 (b), H-N-500 (c) and H-N-700 (d)

Fig. 5: Catalytic activity test data for methane flameless combustion under identical reaction conditions: τ = W/F = 2.5 g_{cat}•h/overall gas flowrate, feeding gas mixture: 20 cm^3/min of 0.5 vol% CH_4, 49.5 vol% He and 50 vol% air: (▲) H-N-500; (♦) H-N-700; (Δ) H-Ac-500; (◇) H-Ac-700)

Fig. 6: Thermal stability test data for the catalysts: (▲) H-N-500; (♦) H-N-700; (Δ) H-Ac-500; (◇) H-Ac-700.

Fig. 7: Typical SEM micrographs of the finished catalysts honeycomb walls after the accelerated thermal deactivation test (Fig.6). Notice the deeper cracks and the worse anchoring of the platelets for the catalyst prepared with La oxide primer from acetate (samples H-Ac-500, Fig.7a and H-Ac-700, Fig.7b, respectively), with respect to the much more compact and less cracked active phase layer of the catalyst prepared with primer from La nitrate (samples H-N-500 and H-N-700, Fig.7c and 7d, respectively).

Fig.1

a)

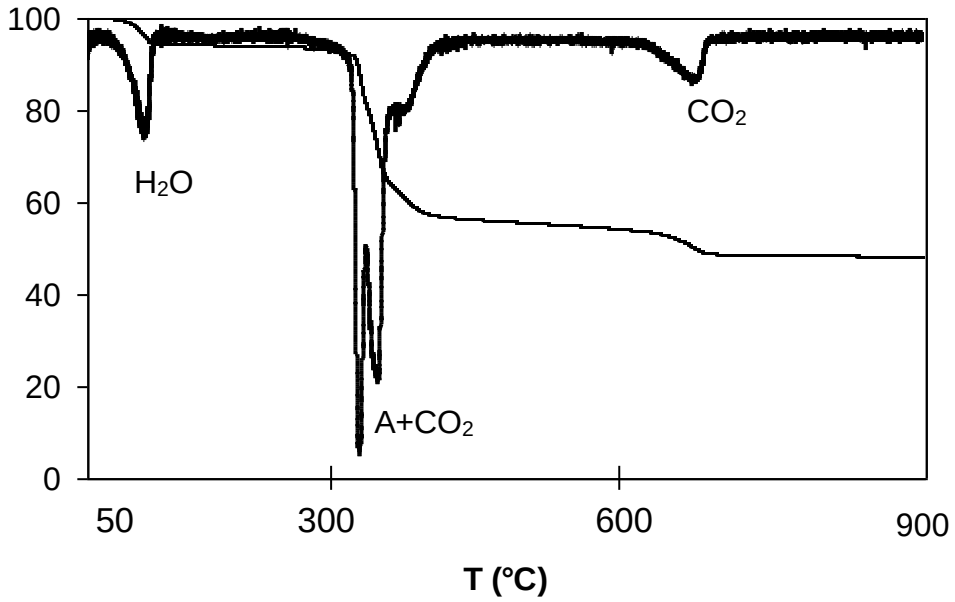
100
80
60
40
20
0
50
300
600
900
T (°C)
H2O
A+CO2
CO2

b)

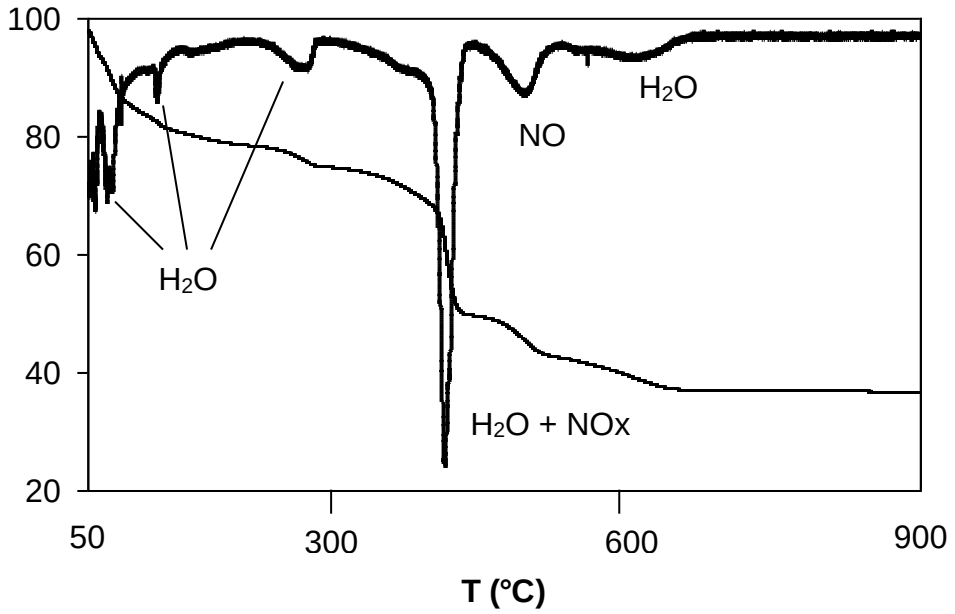
100
80
60
40
20
50
300
600
900
T (°C)
H2O
NO
H2O
H2O + NOx

Fig.2

a)

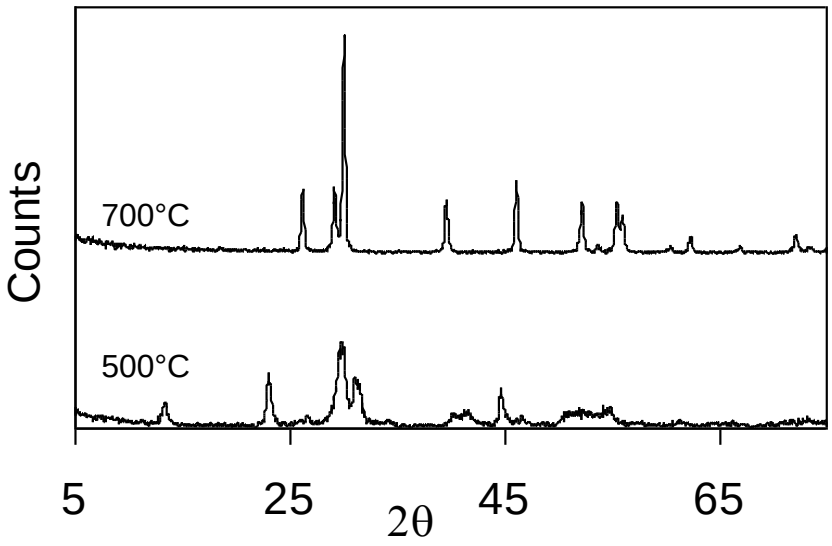

b)

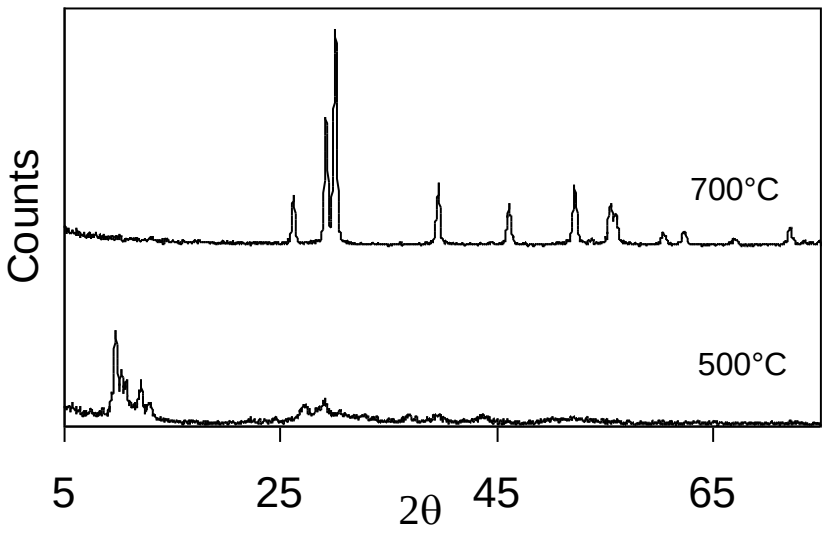

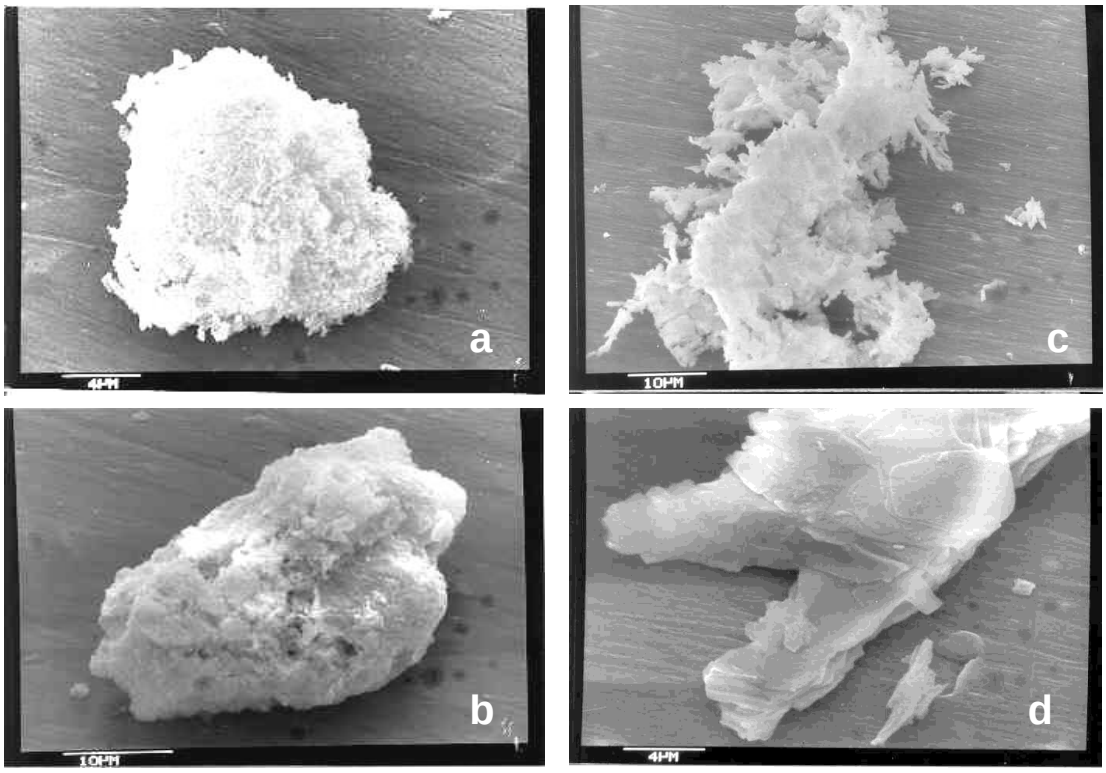

Fig. 3

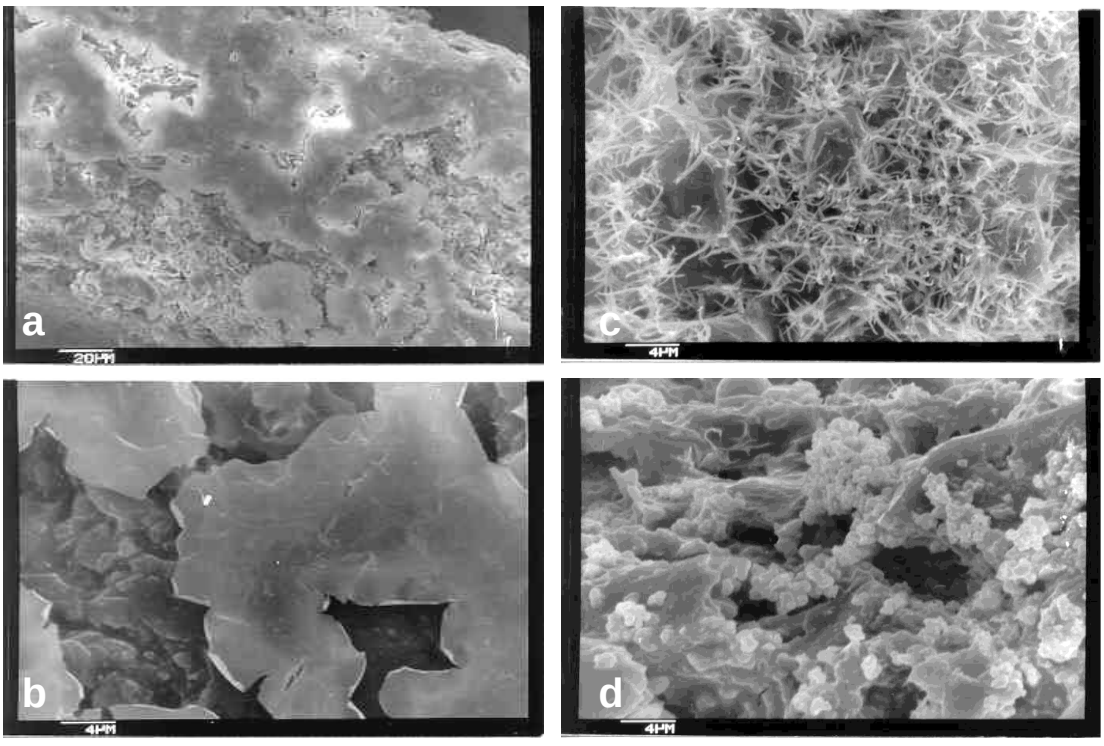

Fig. 4

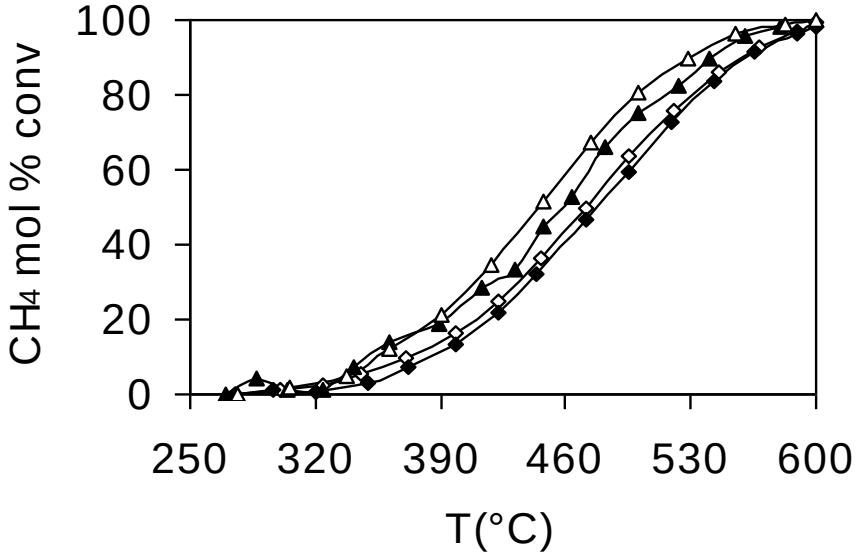
100
80
60
40
20
0
CH4 mol % conv
250
320
390
460
530
600
T(°C)

Fig. 5

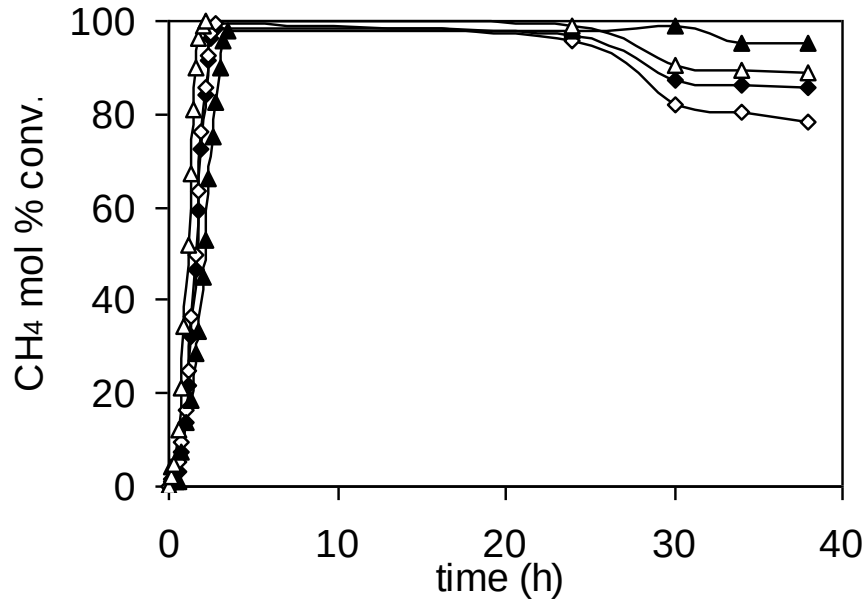
100
80
60
40
20
0
CH4 mol % conv.
0
10
20
30
40
time (h)

Fig. 6

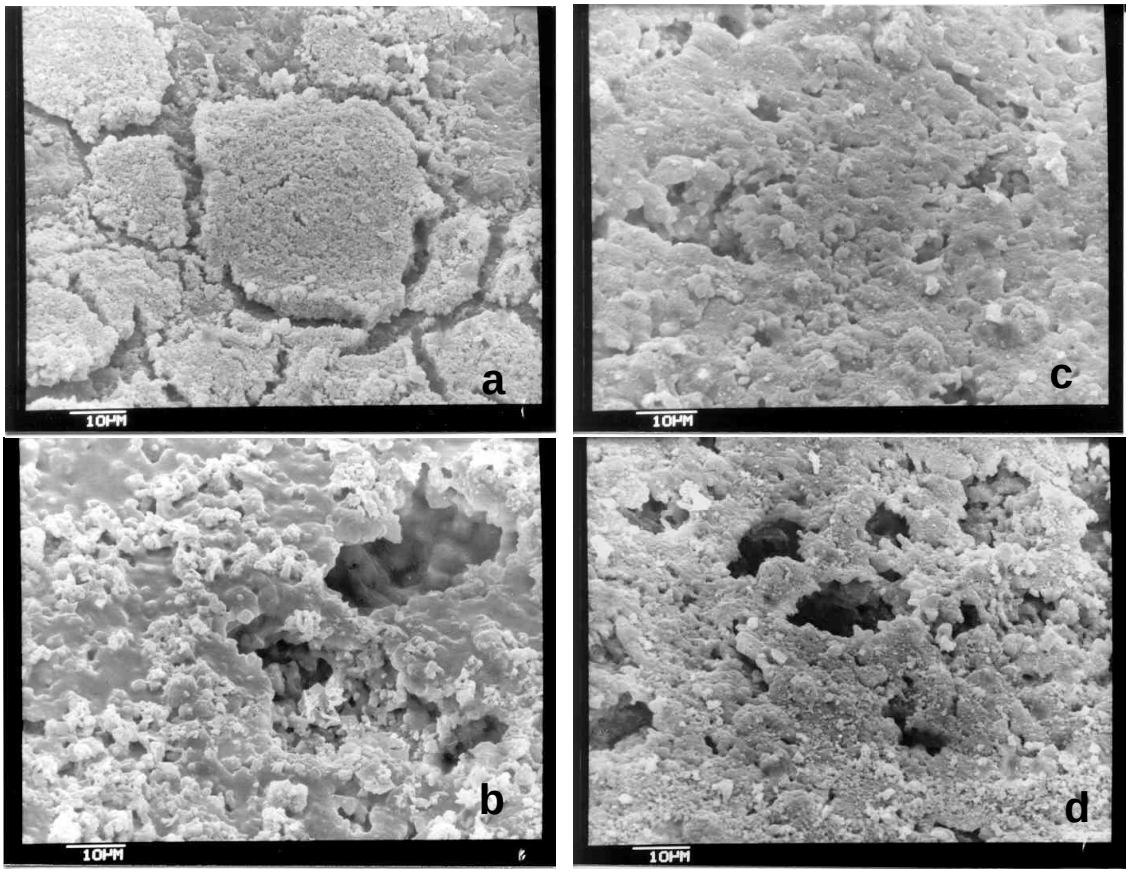

Fig. 7